Asian Journal of Chemistry; Vol. 34, No. 12 (2022), 3320-3326

ASIAN JOURNAL OF CHEMISTRY

https://doi.org/10.14233/ajchem.2022.23983

Binary Mixture of *t*(3)-Methyl-*r*(2),*c*(6)-diphenyl-piperidin-4-one and Gum Exudates of *Astragalus genus* as an Green Soldier for Dissolution Control of Mild Steel in HCl

T. BRINDHA[1], R. RATHINAM[2], S. DHEENADHAYALAN[3,*], S. SUPRIYA[4] and S. MADHANKUMAR[3]

[1]Department of Science and Humanities, Faculty of Engineering, Karpagam Academy of Higher Education (Deemed to be University), Coimbatore-641021, India
[2]Department of Science and Humanities, Sri Eshwar College of Engineering, Coimbatore-641202, India
[3]Department of Chemistry, Erode Sengunthar Engineering College, Erode-638057, India
[4]Department of Chemistry, Jansons Institute of Technology, Coimbatore-641659, India

*Corresponding author: E-mail: vsdheena@gmail.com

Received: 27 June 2022; *Accepted*: 22 October 2022; *Published online*: 25 November 2022; AJC-21063

The corrosion inhibitive behaviour of *t*(3)-Methyl-*r*(2),*c*(6)-diphenyl-piperidin-4-one (3MDPP) and gum exudates of Astragalus genus (GTP) on mild steel in 1 N HCl were studied using weight loss measurements for 1 h immersion period at 303-323 K. The corrosion rate of mild steel directly varies with temperature whereas it varies inversely with concentration. The synergistic influence of different concentrations of GTP on 3MDPP was analyzed at 303-323 K using weight loss technique. The i_{corr}, E_{corr}, R_{ct} and C_{dl} values were obtained for 3MDPP, GTP and the mixture of GTP and 3MDPP (binary mixture). The calculated values of E_a, ΔH^*, ΔS^* and ΔG°_{ads} suggests the physical adsorption mechanism and it obeys Langmuir isotherm. The synergistic influence of GTP on 3MDPP is clear from the synergistic parameter value (> 1).

Keywords: Mild steel, *t*(3)-Methyl-*r*(2),*c*(6)-diphenyl-piperidin-4-one, Astragalus genus, Gum, Binary mixture, Synergism.

INTRODUCTION

Nowadays most of the countries and their industries concern for the development of corrosion control of metal and alloy. Mostly aggressive acids (HCl, H_2SO_4) are employed for acid pickling, chemical cleaning, ore separation and oil well cleaning. During these processes, metallurgical properties of metals are affected by means of corrosion [1]. To minimize the corrosion, certain inorganic salts such as nitrates, phosphates, chromates, molybdates, *etc.* and organic compounds containing hetero-atoms with multiple bonds are used as effective inhibitors in acidic medium [2-7]. Currently, there is an increasing quest for limiting field applications involving toxic compounds, hence the search for greener alternatives by reformulating the existing organic compounds or by developing safer products [8-13].

Accordingly, the main goal of present work has been proposed, to synthesize a piperidone derivative, *t*(3)-Methyl-*r*(2),*c*(6)-diphenyl-piperidin-4-one (3MDPP) and to investigate their influence on the corrosion inhibition of mild steel in 1 N HCl using quantitative (gravimetry) and qualitative (electrochemical) methods. At higher temperature, the stability and corrosion inhibition performance of 3MDPP on mild steel in 1 N HCl are reformulating by the use of non-toxic green adhesive such as natural gum exudates. A thorough survey of literature reveals that no work has so far been done on the influence of plant gum exudates such as *Astragalus genus* also known as gum tragacanth powder (GTP) as natural synergist for corrosion inhibition behaviour of 3MDPP. Therefore, the synergistic corrosion inhibition and thermodynamic adsorption behaviour between 3MDPP and GTP for mild steel corrosion in 1 N HCl medium was investigated using weight loss, potentiodynamic polarization and electrochemical impedance spectroscopic methods for 1 h immersion period at 303-323 K. The inhibitive effect of GTP on mild steel in 1 N HCl at 303-323 K is also a part of this investigation.

EXPERIMENTAL

Mild steel rectangular specimens (0.0460 wt.% C, 0.28 wt.% Mn, 0.019 wt.% P, 0.020 wt.% S, 0.006 wt.% Si and rest

of iron) of dimension 2.5 cm × 1.0 cm × 0.1 cm was used for the study. Different grades of emery sheets were used to polish the mild steel surface and degreased with ethanol, air-dried at 30 ºC and stored in a moisture free desiccator. Laboratory grade HCl was used as an aggressive medium. The commercially available purified gum exudates of Astragalus genus (GTP) was used for the present study. The gum was dissolved using deionized water and used for electrochemical and non-electrochemical studies. The 3MDPP was synthesized using the reported procedure [14,15].

Gravimetric method: The gravimetric data were obtained according to the ASTM methods [16]. The pre-cleaned samples were weighed and immersed in 1 N HCl with and without, various concentrations of 3MDPP, GTP and binary mixture for 1 h at 303-323 K. After 1 h immersion, the mild steel plates were taken out and treated with clark solution for 40 s, rinsed with deionized water and followed by ethanol, dried in hot air and then weighed. From the weight loss, the following parameters are calculated using equation eqns. 1-3:

$$\text{Corrosion rate } (C_R) = 87.6 \times \frac{W}{\rho \times A \times t} \quad (1)$$

$$\text{Inhibition efficiency } (\%) = \left(\frac{W_o - W_{inh}}{W_o} \right) \times 100 \quad (2)$$

$$\text{Surface coverage } (\theta) = \left(\frac{W_o - W_{inh}}{W_o} \right) \quad (3)$$

where W, ρ, A, t, W_o and W_{inh} represents mass loss (g), density of MS (g cm^{-3}), area of the coupon (cm^2), immersion time (h), weight loss of mild steel without and with inhibitor, respectively.

Tafel's polarization studies: The cell assembly consisting of three electrodes namely saturated calomel electrode (reference electrode) and platinum as counter electrode with the solution capacity of 100 mL was used for electrochemical measurement. A potential range of +200 mV to -200 mV with respect to the OCP at a scan rate of 1 mV s^{-1} was fixed. From the plot of potential *versus* log current, the corrosion potential (E_{corr}) and corrosion current density (i_{corr}), Tafel slopes b_a and b_c were obtained in the blank and inhibited solutions. From the measured i_{corr} values, the inhibition efficiencies of inhibitors obtained using eqn. 4:

$$\text{Inhibition efficiency } (\%) = \left(\frac{i^o_{corr} - i_{corr}}{i^o_{corr}} \right) \times 100 \quad (4)$$

where i^o_{corr} and i_{corr} are the corrosion current density in absence and presence of inhibitor.

Impedance studies: The impedance measurements were done over the frequency range of 10 KHz to 0.01 Hz with AC signal amplitude of 10 mV at the corrosion potential for 30 min of immersion at 30 ºC. The measurements were automatically controlled by Z_{view} software and the impedance diagrams are given as Nyquist plots. From the Nyquist plots, charge transfer resistance (R_{ct}) and double layer capacitance (C_{dl}) were calculated. The inhibition efficiency was calculated using eqn. 5:

$$\text{Inhibition efficiency } (\%) = \left(\frac{R_{ct} - R^o_{ct}}{R_{ct}} \right) \times 100 \quad (5)$$

where R_{ct} and R^o_{ct} are the charge transfer resistance with and without inhibitor.

RESULTS AND DISCUSSION

Gravimetric method

Effect of concentration of 3MDPP: *t*(3)-Methyl-*r*(2), *c*(6)-diphenyl-piperidin-4-one (3MDPP) has been investigated as inhibitor for mild steel corrosion in 1 N HCl using gravimetric method at 303-323 K for 1 h immersion period. The corrosion parameters were derived from weight loss are shown in Table-1, which revealed that 50, 250, 500, 750 ppm of 3MDPP gives 44.82%, 58.39%, 76.79% and 82.04% efficiency, respectively and inhibition efficiency increase with increase in the concentration of 3MDPP and its efficiency attain saturation when the concentration of 3MDPP increased further.

The increasing inhibition efficiency of 3MDPP may be due to presence of carbonyl group and ring nitrogen [17-20]. A protective layer on the mild steel surface was formed due to the interaction of 3MDPP with the mild steel surface. This could occur either through carbonyl group or non-bonding electrons of ring nitrogen. The interaction of 3MDPP with mild steel surface not through both of them since the molecule is in chair form and the groups are in *para*-position to each other [21]. It is impossible for both groups to participate at once because doing so would require achieving boat conformation, which is extremely difficult. Also the less electronegativity of nitrogen than oxygen favours ring nitrogen to be the inhibiting site. The inhibition efficiency of 3MDPP decreases with rise in temperature, which may be due to desorption of 3MDPP and suggesting the physical adsorption of the 3MDPP on the mild steel.

Effect of GTP concentration at 303-323 K: Gum exudates of Astragalus genus (GTP) has been tested as green inhibitor for mild steel corrosion in 1 N HCl medium for 1 h immersion period at 303-323 K. From the weight loss data, the corrosion

TABLE-1
CORROSION PARAMETERS FOR 3MDPP ON MILD STEEL IN 1 N HCl

Conc. (ppm)	303 K			313 K			323 K		
	IE (%)	CR (mmpy)	θ	IE (%)	CR (mmpy)	θ	IE (%)	CR (mmpy)	θ
Blank		0.0863			0.1560			0.2301	
50	44.82	0.0476	0.4482	25.36	0.1164	0.2536	30.18	0.1607	0.3018
250	58.39	0.0359	0.5839	50.57	0.0771	0.5057	51.70	0.1111	0.5170
500	76.79	0.0200	0.7679	64.86	0.0548	0.6486	67.96	0.0737	0.6796
750	82.04	0.0155	0.8204	77.95	0.0344	0.7795	81.43	0.0427	0.8143

TABLE-2
CORROSION PARAMETERS FOR GTP ON MILD STEEL IN 1 N HCl

Conc. (ppm)	303 K			313 K			323 K		
	IE (%)	CR (mmpy)	θ	IE (%)	CR (mmpy)	θ	IE (%)	CR (mmpy)	θ
Blank		0.0863			0.1560			0.2301	
10	39.56	0.0522	0.3956	32.88	0.1047	0.3288	26.07	0.1701	0.2607
20	53.58	0.0401	0.5358	46.45	0.0835	0.4645	27.38	0.1671	0.2738
40	60.15	0.0344	0.6015	49.60	0.0786	0.4960	45.78	0.1248	0.4578
100	64.09	0.0310	0.6409	61.23	0.0605	0.6123	47.26	0.1214	0.4726

parameters were derived and presented in Table-2. The data analysis clearly shows that the inhibition efficiency improves with increase in concentrations of GTP from 10 ppm to 100 ppm and maximum efficiency was achieved at 100 ppm of GTP (52.01%).

The GTP is mixture of polysaccharides of high molecular weight carbohydrate biopolymer and also it consists of trace amount of proteins in its composition. These carbohydrate biopolymers undergoes hydrolysis in the testing solution (1 N HCl) and produce monomers of carbohydrates units such as (D)-galacturonic acid, (D)-galactose, (L)-fucose, (D)-xylose, (L)-arabinose, (L)-rhamnose, *etc*. These molecules are electrochemically active and interact with the mild steel surface through their labile electrons resulting in the formation of a superamolecular structure. Due to polymeric nature and very good adhesive property of GTP, the formed superamolecular complexes on mild steel are stable and rapidly occupy greater surface area on mild steel resulting in enhanced inhibition efficiency. But the inhibition efficiency of GTP slightly decreases by increasing the temperature from 303-313 K. But the inhibition efficiency is only slightly altered at 323 K. This indicates the physical adsorption nature.

Synergistic influence of GTP on 3MDPP: The synergistic corrosion inhibition is an effective means of improving the inhibition nature and decreasing the amount of usage of inhibitors [22-24]. The synergistic influence of optimum concentration of 20 ppm of GTP on the corrosion inhibition behaviour of various concentrations (50, 250, 500, 750 ppm) of 3MDPP towards mild steel corrosion in 1 N HCl medium has been investigated using gravimetric method at 303 K for 1 h immersion period. The result of weight loss of mild steel with and without binary mixture in 1 N HCl were used to evaluated their corrosion kinetic and synergistic parameters. Table-3 revealed that the corrosion protection efficiency of various concentrations of 3MDPP (50, 250, 500, 750 ppm) together with 20 ppm of GTP on mild steel in 1 N HCl are significantly enhanced greater percentage than individual components. Also their corrosion rate significantly very less for this combination of binary mixture system. This is mainly due to the synergism existing between 3MDPP and GTP.

The reason can be explained as initially 3MDPP present in the binary mixture acted as effective nucleophile [25] and it is rapidly adsorbed on the mild steel surface through strong force of electrostatic interactions existing with Fe^{2+} ions of mild steel surface and labile electrons of ring nitrogen atom of 3MDPP. This adsorbed 3MDPP molecules act as intermediate bridge between mild steel surface and GTP. If the medium is non-aqueous, 3MDPP will form a strong bond with Fe^{2+} but in aqueous medium water molecules are competing with 3MDPP to form coordinate type bond [25,26]. Hence, the inhibition efficiency is only 45% at room temperature. But in presence of GTP, a strong intermolecular hydrogen bonding is formed between the ring carbonyl oxygen atom of adsorbed 3MDPP molecule (lying *para* to ring nitrogen atom) and hydrolyzed monomeric units of –OH or –COOH or $–NH_2$ groups of GTP and prevents the outward moment (desorption) of 3MDPP from the mild steel surface. This type of interaction between adsorbed 3MDPP and monomers of GTP enhance the stability of mild steel in aggressive medium through stabilization of positive charge of mild steel surface in 1 N HCl. The effect of temperature on the inhibition efficiency of binary inhibitor is evaluated by performing the weight loss experiments at 313 and 323 K (Table-3). The inhibition efficiency of various concentrations of 3MDPP with 20 ppm of GTP is slightly decreases with increase in temperature. Compared to individual components the rate of dissolution of mild steel is also very less at higher temperature. This may be due to hydrolyzing ability of GTP in 1 N HCl. At higher temperature, the more number of carbohydrates and proteins monomers are produced in the tested solution, resulting in the enhancement of the thickness of adsorbed protective layer to a greater percentage on mild steel surface. Table-3 clearly reveals that the inhibition efficiency given by 750 ppm of 3MDPP along with 20 ppm of GTP is around 91.24% and stable up to 313 K. This is again due to intermolecular hydrogen bond formation between 3MDPP and GTP, which becomes stable at higher temperature. The gum

TABLE-3
CORROSION PARAMETERS FOR BINARY MIXTURE ON MILD STEEL IN 1 N HCl

Conc. (ppm)	303 K			313 K			323 K		
	IE (%)	CR (mmpy)	S_θ	IE (%)	CR (mmpy)	S_θ	IE (%)	CR (mmpy)	S_θ
Blank		0.0863			0.1560			0.2301	
50	69.78	0.0261	1.42	62.44	0.0586	1.15	49.23	0.1168	1.17
250	79.42	0.0178	1.42	82.79	0.0268	1.17	73.71	0.0605	1.07
500	84.23	0.0136	1.55	86.67	0.0208	1.29	83.41	0.0382	1.14
750	91.24	0.0076	1.49	90.06	0.0155	1.39	87.84	0.0280	1.24

molecules prevent desorption of 3MDPP molecules from the mild steel surface by forming a protective film and hence excellent corrosion protection efficiency. The value of synergistic parameter (S_e) was evaluated using the relationship given by Aramaki *et al*. [27] reveals that the synergistic parameter values were > 1 for all the studied concentrations indicating the pronounced inhibition efficiency resulting from the addition of GTP to 3MDPP. This may be due to attractive force between GTP and 3MDPP on the mild steel surface.

Thermodynamic and kinetic analysis: The corrosion rate of mild steel in 1 N HCl medium is related to temperature and is represented by Arrhenius equation (eqn. 6):

$$\log CR = \log A - \frac{E_a^*}{2.303RT} \quad (6)$$

where CR is the corrosion rate, A is the frequency factor, E_a is the apparent activation energy, R is the universal gas constant and T is the absolute temperature. The plots between log CR and inverse of temperature (1000/T) gave a perfect straight line (Fig. 1). From the slope, the values of E_a can be calculated. The values of ΔH^* and ΔS^* are calculated using the transition state equation (eqn. 7):

$$CR = \left(\frac{RT}{Nh}\right)\exp\left(\frac{\Delta S^*}{R}\right)\exp\left(\frac{-\Delta H^*}{RT}\right) \quad (7)$$

where N is the Avogadro number, h is the Planck constant, ΔS^* is the entropy of activation and ΔH^* is the Enthalpy of activation. Fig. 2 represents the plot of log (CR/T) *vs*. (1000/T) gave straight line with slope ($-\Delta H^*/2.303R$) and intercept [log (R/Nh) + ($\Delta S^*/2.303R$)], from which ΔH^* and ΔS^* are calculated.

It is evident from Table-4 that the apparent activation energy (E_a) increased in inhibited solution when compared to the uninhibited solutions. This shows that a strong inhibitive action of inhibitors by increasing energy barrier for the corrosion process and it reveals that mode interaction between the mild steel surface and inhibitor molecules should be physical (electrostatic attraction) adsorption process. In general the higher value of E_a in the presence of inhibitors as compared to blank solution indicates physical adsorption whereas unchanged or lower value of E_a for inhibitor compared to blank indicates chemisorption mechanism [28]. The value of ΔH^* is higher in presence of inhibitors compared to blank suggests that there is an increasing energy barrier for the corrosion process of mild steel surface and it supports the physical mode of adsorption process. The positive value of ΔH^* in with and without presence and absence of inhibitor reflects the endothermic nature of mild steel dissolution process. The negative values of ΔS^* and its shift towards more negative in inhibited solution compared to blank suggests that activation complex in the rate determining step is due to association rather than dissociation. This implies that disorderness decreases when going from reactant to the activated state.

TABLE-4
ACTIVATION PARAMETERS FOR 3MDPP, GTP AND BINARY MIXTURE ON MILD STEEL IN 1 N HCl

Inhibitor	Conc. (ppm)	E_a^* (kJ mol^{-1})	ΔH^* (kJ mol^{-1})	$-\Delta S^*$ (J mol^{-1})
GTP	Blank	39.97	37.37	141.89
	10	48.17	45.57	119.01
	20	58.10	55.50	88.67
	40	52.56	49.96	107.79
	100	55.50	52.90	99.48
3MDPP	50	49.72	47.12	114.19
	250	46.14	43.54	128.58
	500	53.31	50.71	109.34
	750	41.50	38.90	150.62
Binary mixture	50	61.05	58.45	82.40
	250	49.67	47.07	123.84
	500	41.90	39.29	151.43
	750	53.29	50.69	118.30

Adsorption isotherm: Both corrosion inhibition performance of 3MDPP, GTP and synergistic inhibition of GTP with 3MDPP (binary mixture) on mild steel in 1 N HCl can be described by the adsorption of the molecules on the surface of mild steel and it is directly proportional to the fraction of the surface covered by the adsorbed molecule (θ). Therefore, the

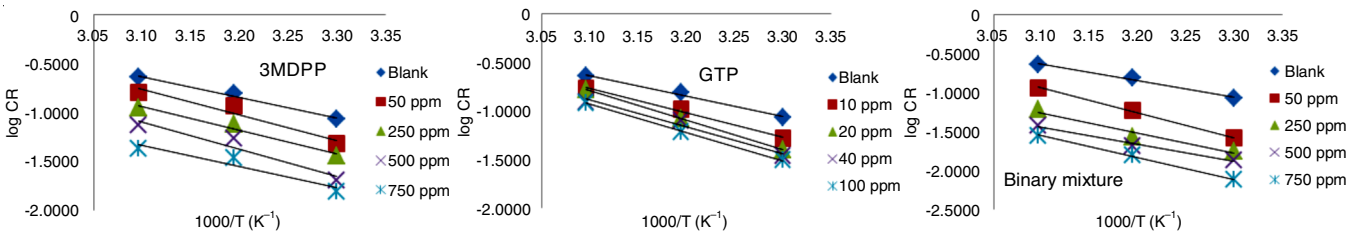

Fig. 1. Arrhenius plots for 3MDPP, GTP and binary mixture on mild steel in 1 N HCl

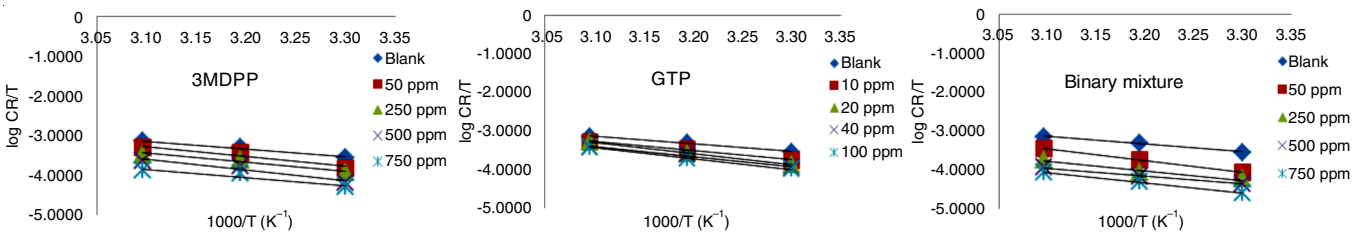

Fig. 2. Transition state plots for 3MDPP, GTP and binary mixture on mild steel in 1 N HCl

adsorption isotherm describes the relationship between the coverage of interface with the adsorbed species and the concentration of species in solution. The surface coverage value (θ) at different concentrations of 3MDPP, GTP and binary mixture in 1 N HCl was tried to fit to various adsorption isotherms (Henry, Frendlich, Langmuir, Frumkin and Temkin isotherms). The regression coefficients (R^2) were used to confirm the best fit. The adsorption of studied inhibitor system on mild steel obeys Langmuir isotherm and it is represented as (eqn. 8):

$$\frac{C_{inh}}{\theta} = \frac{1}{K_{ads}} + C_{inh} \quad (8)$$

where, K_{ads} is the equilibrium constant. The ΔG°_{ads} was calculated from eqn. 9:

$$K = -\log C_{H_2O} - \left(\frac{\Delta G^{\circ}_{ads}}{2.303RT}\right) \quad (9)$$

The Langmuir's plot (Fig. 3) for tested inhibitor systems gave a straight line which indicates the monolayer adsorption. From the intercept of the plot, the values of K_{ads} were obtained which is used to calculate the values of ΔG°_{ads} (Table-5). In general, the values of ΔG°_{ads} of the order of -20 kJ mol^{-1} or lower indicate a physisorption while those more negative than -40 kJ mol^{-1} involve sharing or transfer of electrons from the inhibitor molecules to the metal surface to form a coordinate type of bond [29]. It is clear from the Table-5 that the calculated ΔG°_{ads} values are in the range between -14.37 and -16.05 kJ mol^{-1} for 3MDPP and between -19.56 and -21.99 kJ mol^{-1} for GTP. The ΔG°_{ads} value for binary mixture in the range of -17.24 and -18. 91 kJ mol^{-1}. These results proved that 3MDPP and GTP adsorption on the mild steel surface is a physisorption process; however, in the binary mixing system, 3MDPP and GTP create a strong layer on the mild steel surface.

TABLE-5
ADSORPTION PARAMETERS FOR 3MDPP, GTP AND BINARY MIXTURE ON MILD STEEL IN 1 N HCl

Inhibitor	Temp. (K)	Intercept	K (mol^{-1})	$-\Delta G^{\circ}_{ads}$ (kJ mol^{-1})
GTP	303	0.0090	111.0834	21.99
	313	0.0163	61.2945	20.49
	323	0.0236	42.3287	19.56
3MDPP	303	0.0950	10.5233	16.05
	313	0.1849	5.4088	14.37
	323	0.1647	6.0704	14.66
Binary mixture	303	0.0344	29.0333	18.61
	313	0.0305	32.7473	18.91
	323	0.0592	16.8973	17.24

Electrochemical methods

Tafel's polarization studies: The corrosion inhibition properties of 3MDPP, GTP and the synergistic effect between GTP and 3MDPP on mild steel in 1 N HCl understand with the help of polarization studies. Inhibitors are able to change the anodic process or the cathodic process or both resulting in the decreased rate of the corrosion process. Fig. 4 shows the Tafel polarization curves for mild steel carried in 1 N HCl in the presence and absence of optimum concentration of 3MDPP, GTP and binary mixture at room temperature. The polarization parameters i_{corr}, E_{corr}, Tafel slopes (b_a and b_c) were caluculated and presented in Table-6. It is evident from Fig. 4 that all studied inhibitors were found to block the electrochemical processes on mild steel undergoing corrosion. It decreases both the anodic and cathodic reaction rates by lowering the corrosion current densities on both sides of the Tafel polarization curve in the potential region studied and hence decreases the corrosion rate. Moreover, the i_{corr} values gradually decreases by the addition of 3MDPP, GTP and binary mixture. The i_{corr} value is significantly less for the binary inhibitors system and there is no remarkable change in E_{corr} and Tafel slopes values were observed. Generally, the change observed in the Tafel's plots in the presence of inhibitors is used as criteria to categorize inhibitors as cathodic, anodic or mixed types [30]. Therefore, the studied inhibitors are functioning by mixed type inhibition mechanism, predominantly controlled by anodic reaction. This means that 3MDPP, GTP and binary mixture have significant effects on retarding both anodic dissolution of mild steel and inhibiting the cathodic hydrogen evolution. The i_{corr} values obtained from the Tafel's plots were also used to determine inhibition efficiency

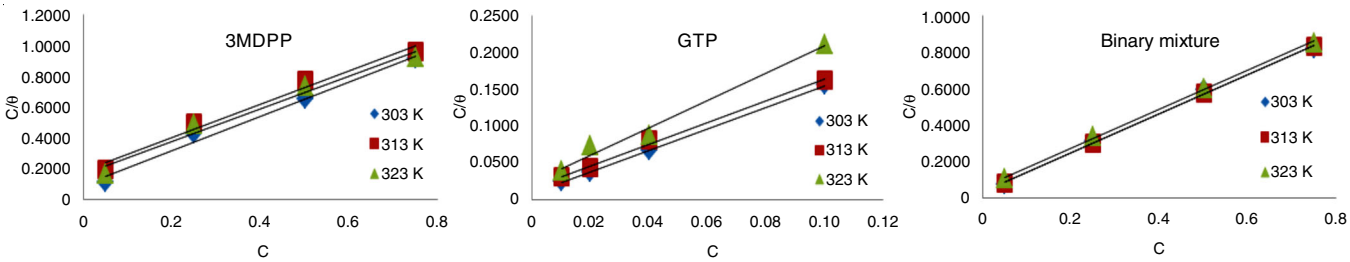

Fig. 3. Langmuir isotherms plots for 3MDPP, GTP and binary mixture on mild steel in HCl

TABLE-6
POLARIZATION PARAMETERS FOR 3MDPP, GTP AND BINARY MIXTURE ON MILD STEEL IN 1 N HCl

Concentration	i_{corr} (mV/cm^{-2}) × 10^{-4}	E_{corr} (mV/SCE)	b_a (mV/dec)	b_c (mV/dec)	IE (%)
Blank	5.65	-0.4653	0.080	0.134	
50 ppm 3MDPP	3.78	-0.4668	0.073	0.138	33.09
20 ppm GTP	3.58	-0.4523	0.072	0.129	36.63
50 ppm 3MDPP + 20 ppm GTP	2.59	-0.4571	0.068	0.129	54.15

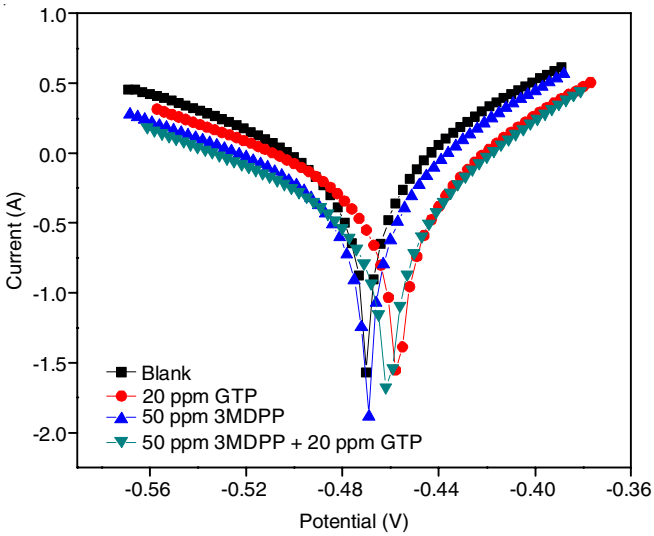

Fig. 4. Tafel's curves for 3MDPP, GTP and binary mixture on mild steel in 1 N HCl

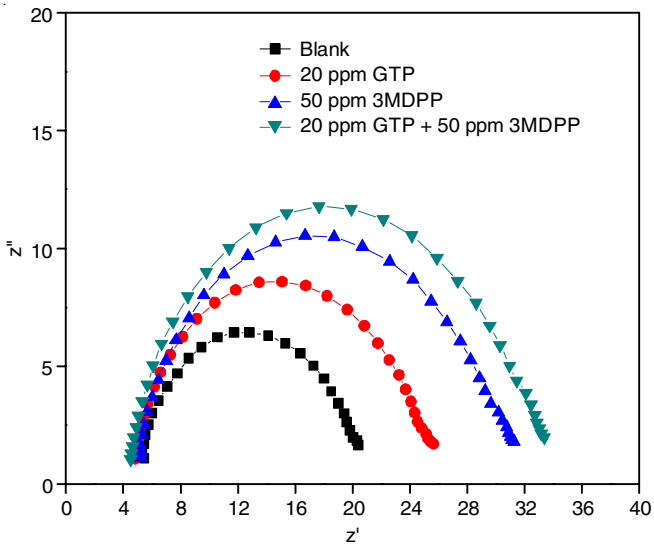

Fig. 5. Nyquist plots for 3MDPP, GTP and binary mixture on mild steel in 1 N HCl

(Table-6). The percentages of inhibition efficiency obtained are analogous with weight loss method. But some deviation could be attributed to the fact that in polarization studies, immediate corrosion current is measured whereas in weight loss experiments the efficiency was calculated after 1 h immersion period.

Impedance studies: The nature of inhibition process of 3MDPP, GTP and synergistic effect between GTP and 3MDPP were also studied by electrochemical impedance spectroscopy technique. The value of R_{ct} is a measure of electron transfer across the surface and inversely proportional to corrosion rate. The value of R_{ct} increases and C_{dl} value decreases when the protective film formed on the surface of mild steel. Impedance measurements in the Nyquist format (Fig. 5) for mild steel in 1 N HCl in absence and presence of optimum concentrations of 3MDPP, GTP and binary mixture are presented in Table-7. The sudden decrease in C_{dl} value for the binary mixture may be attributed to the decrease in local dielectric constant and/or an increase in the thickness of the electric double layer. A decrease in C_{dl} value may also due to the maximum increase in the adsorption inhibitor molecules, which resulted in the enhancement of the inhibition potency. Gradual replacement of water molecules by the adsorption of 3MDPP, GTP and its mixture on the mild steel surface reduce the rate of dissolution of mild steel and consequently, it causes a decrease in C_{dl} values. Using the R_{ct} values, the inhibition efficiency were determined and presented in Table-7. The inhibition efficiency obtained by this method was in good agreement with weight loss data.

Conclusion

In summary, the behaviour of *t*(3)-Methyl-*r*(2),*c*(6)-diphenylpiperidin-4-one (3MDPP) and gum exudates of Astragalus genus (GTP) on mild steel were acted as good corrosion inhibitor for the mild steel corrosion in 1 N HCl were studied. It was found their inhibition efficiency increases with increasing the concentrations of both 3MDPP and GTP and decreases with rise in temperature. Moreover, the binary mixture shows a good efficiency and surface coverage to a greater percentage than

TABLE-7
IMPEDANCE PARAMETERS FOR 3MDPP, GTP AND BINARY MIXTURE ON MILD STEEL IN 1 N HCl

Concentration	R_{ct} (Ω cm^{-2})	C_{dl} (μF cm^{-2})	IE (%)
Blank	14.80	0.0016447	–
50 ppm 3MDPP	26.02	0.0005782	43.12
20 ppm GTP	20.92	0.0008789	29.25
50 ppm 3MDPP + 20 ppm GTP	28.83	0.0004678	48.66

when the inhibitors present alone. The calculated values of E_a, ΔH^* and ΔG°_{ads} for 3MDPP, GTP and binary inhibitors systems conclude a physisorption mechanism and it obeys Langmuir's adsorption isotherm, whereas the Tafel's polarization study reveals that tested inhibitors act as mixed type. Furthermore, the impedance measurements confirmed that a protective film was formed on the mild steel surface in the presence of 3MDPP, GTP and binary mixture.

CONFLICT OF INTEREST

The authors declare that there is no conflict of interests regarding the publication of this article.

REFERENCES

1. Y. Xu, Y. Xu, Y. Zhang, Y. Shu, H. Song, X. Shu, Y. Ma, L. Hao, X. Zhang, X. Ren, Z. Wang and X. Zhang, *ACS Omega*, **7**, 13826 (2022); https://doi.org/10.1021/acsomega.2c00121
2. C. Verma, E.E. Ebenso, M.A. Quraishi and C.M. Hussain, *Mater. Adv.*, 2, 3806 (2021); https://doi.org/10.1039/D0MA00681E
3. A.I. Muñoz, J. García-Antón, J.L. Guiñón and V. Pérez-Herranz, *Electrochim. Acta*, **50**, 957 (2004); https://doi.org/10.1016/j.electacta.2004.07.048
4. P.B. Raja, M. Ismail, S. Ghoreishiamiri, J. Mirza, M.C. Ismail, S. Kakooei and A.A. Rahim, *Chem. Eng. Commun.*, **203**, 1145 (2016); https://doi.org/10.1080/00986445.2016.1172485
5. S.K. Ahmed, W.B. Ali and A.A. Khadom, *Int. J. Indus. Chem.*, **10**, 159 (2019); https://doi.org/10.1007/s40090-019-0181-8
6. K. Parameswari, S. Rekha, S. Chitra and E. Kayalvizhy, *Port. Electrochim. Acta*, **28**, 189 (2010); https://doi.org/10.4152/pea.201003189

7. A.C. Bastos, M.G. Ferreira and A.M. Simões, *Corros. Sci.*, **48**, 1500 (2006); https://doi.org/10.1016/j.corsci.2005.05.021
8. S.A. Umoren, I.B. Obot, E.E. Ebenso and N. Obi-Egbedi, *Desalination*, **247**, 561 (2009); https://doi.org/10.1016/j.desal.2008.09.005
9. H.-M. Yang, *Molecules*, **26**, 3473 (2021); https://doi.org/10.3390/molecules26113473
10. L.T. Popoola, *Corros. Rev.*, **37**, 71 (2019); https://doi.org/10.1515/corrrev-2018-0058
11. S.A. Umorena, I.B. Obota, E.E. Ebenso and N. Obi-Egbedi, *Port. Electrochim. Acta*, **26**, 199 (2008); https://doi.org/10.4152/pea.200802199
12. S. Marzorati, L. Verotta and S.P. Trasatti, *Molecules*, **24**, 48 (2019); https://doi.org/10.3390/molecules24010048
13. S.A. Umoren and U.M. Eduok, *Carbohydr. Polym.*, **140**, 314 (2016); https://doi.org/10.1016/j.carbpol.2015.12.038
14. M.B. Balasubramanian and N. Padma, *Tetrahedron*, **19**, 2135 (1963); https://doi.org/10.1016/0040-4020(63)85028-0
15. C.R. Noller and V. Baliah, *J. Am. Chem. Soc.*, **70**, 3853 (1948); https://doi.org/10.1021/ja01191a092
16. ASTM Practice Standard G-31, Standard Practice for Laboratory Immersion Corrosion Testing of Metals, ASTM International (2004).
17. S. Muralidharan, R. Chandrasekar and S.V.K. Iyer, *Proc. Indian Acad. Sci.*, **112**, 127 (2000); https://doi.org/10.1007/BF02704314
18. A.N. Senthilkumar, K. Tharini and M.G. Sethuraman, *J. Mater. Eng. Perform.*, **20**, 969 (2011); https://doi.org/10.1007/s11665-010-9719-9
19. S. Sankarapapavinasam, F. Pushpanaden and M.F. Ahmed, *Corros. Sci.*, **32**, 193 (1991); https://doi.org/10.1016/0010-938X(91)90043-O
20. A.N. Senthilkumar, K. Tharini and M.G. Sethuraman, *Surf. Rev. Lett.*, **16**, 141 (2009); https://doi.org/10.1142/S0218625X09012408
21. K. Selvaraj, M. Narasimhan and J. Mallika, *Transition Met. Chem.*, **26**, 224 (2001); https://doi.org/10.1023/A:1007144601982
22. S.A. Umoren, Y. Li and F.H. Wang, *Corros. Sci.*, **52**, 1777 (2010); https://doi.org/10.1016/j.corsci.2010.01.026
23. A.M. Ridhwan, A.A. Rahim and A.M. Shah, *Int. J. Electrochem. Sci.*, **7**, 8091 (2012).
24. Q. Hu, Y. Qiu, G. Zhang and X. Guo, *Open Mater. Sci. J.*, **8**, 31 (2014); https://doi.org/10.2174/1874088X01408010031
25. G. Tharial Xavier, B. Thirumalairaj and M. Jaganathan, *Int. J. Corros.*, **2015**, 410120 (2015); https://doi.org/10.1155/2015/410120
26. B. Thirumalairaj and M. Jaganathan, *Egypt. J. Petrol.*, **25**, 423 (2016); https://doi.org/10.1016/j.ejpe.2015.09.002
27. K. Aramaki, M. Hagiwara and H. Nishihara, *Corros. Sci.*, **27**, 487 (1987); https://doi.org/10.1016/0010-938X(87)90092-8
28. M. Mobin and S. Masoor, *Int. J. Electrochem. Sci.*, **7**, 6920 (2012).
29. S.A. Umoren, *Port. Electrochem. Acta*, **27**, 565 (2009); https://doi.org/10.4152/pea.20090556
30. N.O. Eddy and E.E. Ebenso, *Afr. J. Pure Appl. Chem.*, **2**, 46 (2008).